Supporting Information for the

UV photolytic study of thiourea and its N-methylated derivative in cryogenic matrices

Sándor Góbi*,[1,2] Barbara Keresztes,[1,3] Anita Schneiker,[1,3] and György Tarczay[1,2,4]

[1)] *Laboratory of Molecular Spectroscopy, Institute of Chemistry, ELTE Eötvös Loránd University, PO Box 32, H-1518 Budapest, Hungary*

[2)] *MTA-ELTE Lendület Laboratory Astrochemistry Research Group, Institute of Chemistry, ELTE Eötvös Loránd University, PO Box 32, H-1518 Budapest, Hungary*

[3)] *Hevesy György PhD School of Chemistry, Institute of Chemistry, ELTE Eötvös Loránd University, PO Box 32, H-1518 Budapest, Hungary*

[4)] *Centre for Astrophysics and Space Science, ELTE Eötvös Loránd University, PO Box 32, H-1518 Budapest, Hungary*

(*sandor.gobi@ttk.elte.hu)

(Dated: 13 February 2024)

TABLE S1: The main experimental vibrational frequencies of TU thione tautomer isolated in solid Ar and *para*-H_2 matrices as well as values taken from the literature.

Vibrational mode[a]	**Ar**[b]	**Ar**[c]		***para*-H_2**[b]	***normal*-H_2**[c]	
	$\tilde{\nu}$[d]	$\tilde{\nu}$[d]	I[e]	$\tilde{\nu}$[d]	$\tilde{\nu}$[d]	I[e]
Q1, Q2	3538.8	3539	172	3547.6, <u>3545.1</u>	3546	118
Q3	3424.4	3424	47	3432.6, <u>3430.7</u>	3432	28
Q4	3417.6	3418	67	3426.1, <u>3424.3</u>	3425	79
Q5	1610.5	1610	71	1614.5	1612	83
Q6	<u>1589.8</u>, 1581.2	<u>1590</u>, 1581	152	1590.3	1593	224
	1518.6	1518	6	1520.6	1518	6
Q7	1401.2	1401	96	1407.2	1412	84
Q8	1389.0, <u>1384.5</u>	1389, <u>1385</u>	384	1390.9	1391	352
	1272.7	1273	1	1274.8	1282, 1274	3
	1191.9	1192	9	1200.5b	1204	6
	1078.3	1078	7	1085.8b	1088	3
Q10	1043.3	1043	74	1047.6	1050	68
Q9	1023.9	1024	12	1030.8b	1032	13
Q11	759.8	760	16	760.9	759	16
Q13	712.1	712	28	–	749	20
Q14	644.4	645	29	–	688	12

[a] for an approximate description and PED analysis, see Ref. 1

[b] this work

[c] data taken from Ref. 2

[d] in cm^{-1}; b: broad; more intense components of split bands are underlined

[e] relative integrated intensities

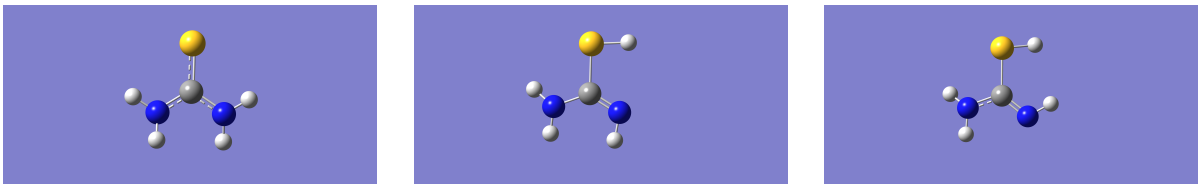

FIG. S1: Structures of the thione (left), the *s,t*- (middle), and the *s,c*-thiol (right) tautomers of TU.

TABLE S2: The main experimental vibrational frequencies of the *s,t*-thiol tautomer of TU isolated in solid Ar and *para*-H_2 matrices as well as values taken from the literature.

Vibrational mode[a]	**Ar**[b]	**Ar**[c]		***para*-H_2**[b]	***normal*-H_2**[c]	
	$\tilde{\nu}$[d]	$\tilde{\nu}$[d]	I[e]	$\tilde{\nu}$[d]	$\tilde{\nu}$[d]	I[e]
Q1	3519.7	3520	68	3530.2	3529	18
Q2	3419.2	3419	27	–	3427	35
Q4	2624.9?	2625	13	2618.1	2619	10
Q5	1640.6	1641	293	1643.9	1642	324
Q6	1597.1	1597	68	1598.7	1599	69
	–	–	–	–	1399	20
	1341.6	1342	26	1346.6	1348	18
Q7	1317.7	1318	187	1321.5	1325	146
Q8	1086.2	1086	44	1088.7	1092	52
Q9	1067.1	1067	48	1070.3	1073	60
Q10	888.4	890, <u>888</u>	16	891.4	894	19
Q11	807.3	807	34	–	–	–
	772.6	772	25	–	783	44
Q12	670.6	671	53	673.4	674	43

[a] for an approximate description and PED analysis, see Ref. 1

[b] this work

[c] data taken from Ref. 2

[d] in cm^{-1}; more intense components of split bands are underlined

[e] relative integrated intensities

TABLE S3: The main experimental vibrational frequencies of the *s,c*-thiol tautomer of TU isolated in solid Ar and *para*-H_2 matrices as well as values taken from the literature.

Vibrational mode[a]	**Ar**[b]	**Ar**[c]		***para*-H_2**[b]		***normal*-H_2**[c]
	$\tilde{\nu}$[d]	$\tilde{\nu}$[d]	I[e]	$\tilde{\nu}$[d]	$\tilde{\nu}$[d]	I[e]
Q1	3522.2	3522	84	3527.2	3525	80
Q2	3414.8	3415	39	–	–	–
Q4	2624.9?	2623	6	–	–	–
Q5	1649.2	1649	327	1653.2	1652	235
Q6	–	1580	40	–	–	–
	–	1445	2	1449.8b	1451	147
Q7	1293.8b	1294	149	1298.2b	1300	106
Q8	1120.8b, 1113.1b	1121, 1112	80	1121.0b	–	–
Q9	1076.9	1077	59	1080.2	1084	186
Q10	911.3b	909	16	–	913	26
	829.2b	829	6	–	–	–
Q12	657.3b	658	35	660.0	–	–

[a] for an approximate description and PED analysis, see Ref. 1

[b] this work

[c] data taken from Ref. 2

[d] in cm^{-1}; b: broad; ?: tentative assignment

[e] relative integrated intensities

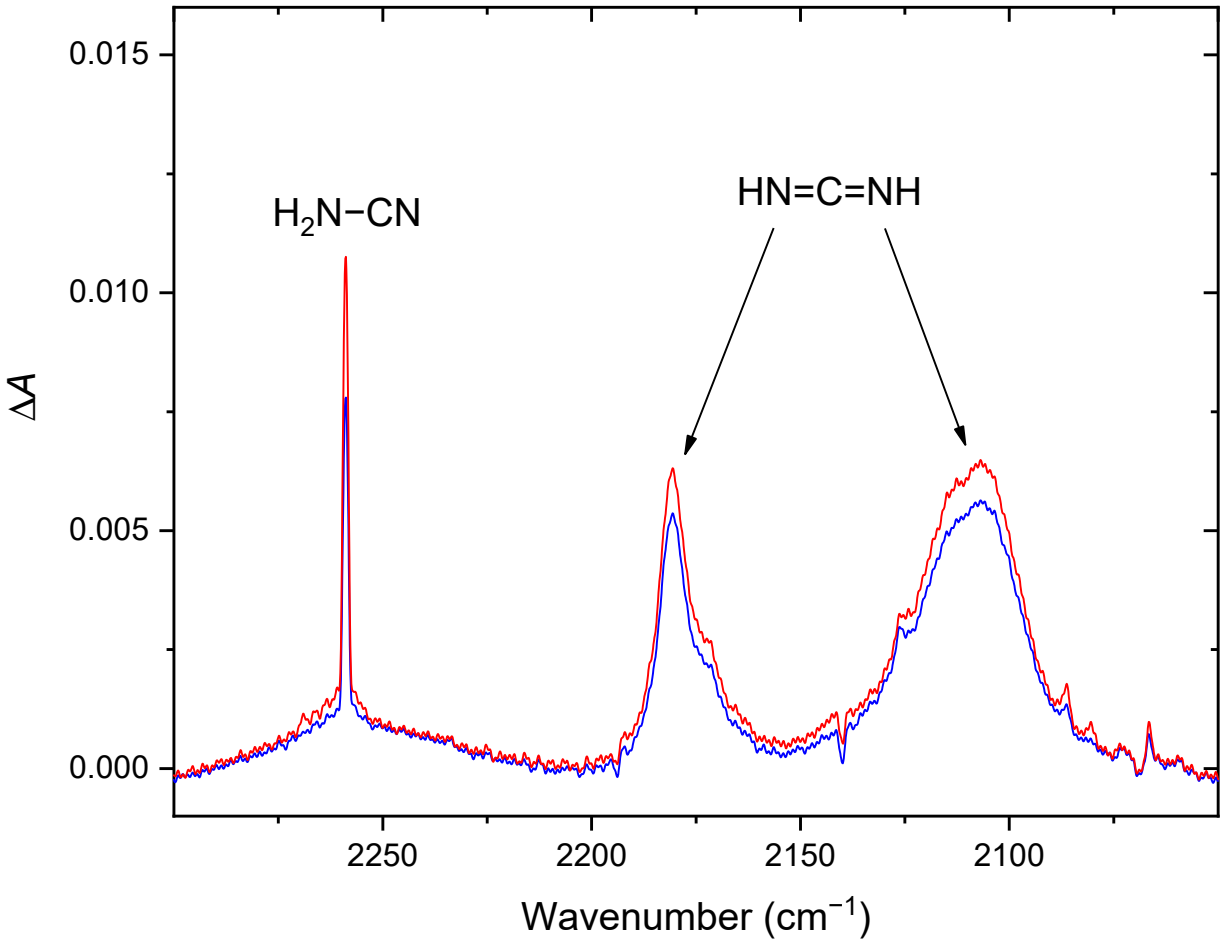

FIG. S2: Difference spectra of the most prominent bands appearing after exposing TU to 240 (blue trace) and 216 nm photons (red) isolated in solid Ar. The reference spectrum was the one taken right before the start of the 240 nm photolysis.

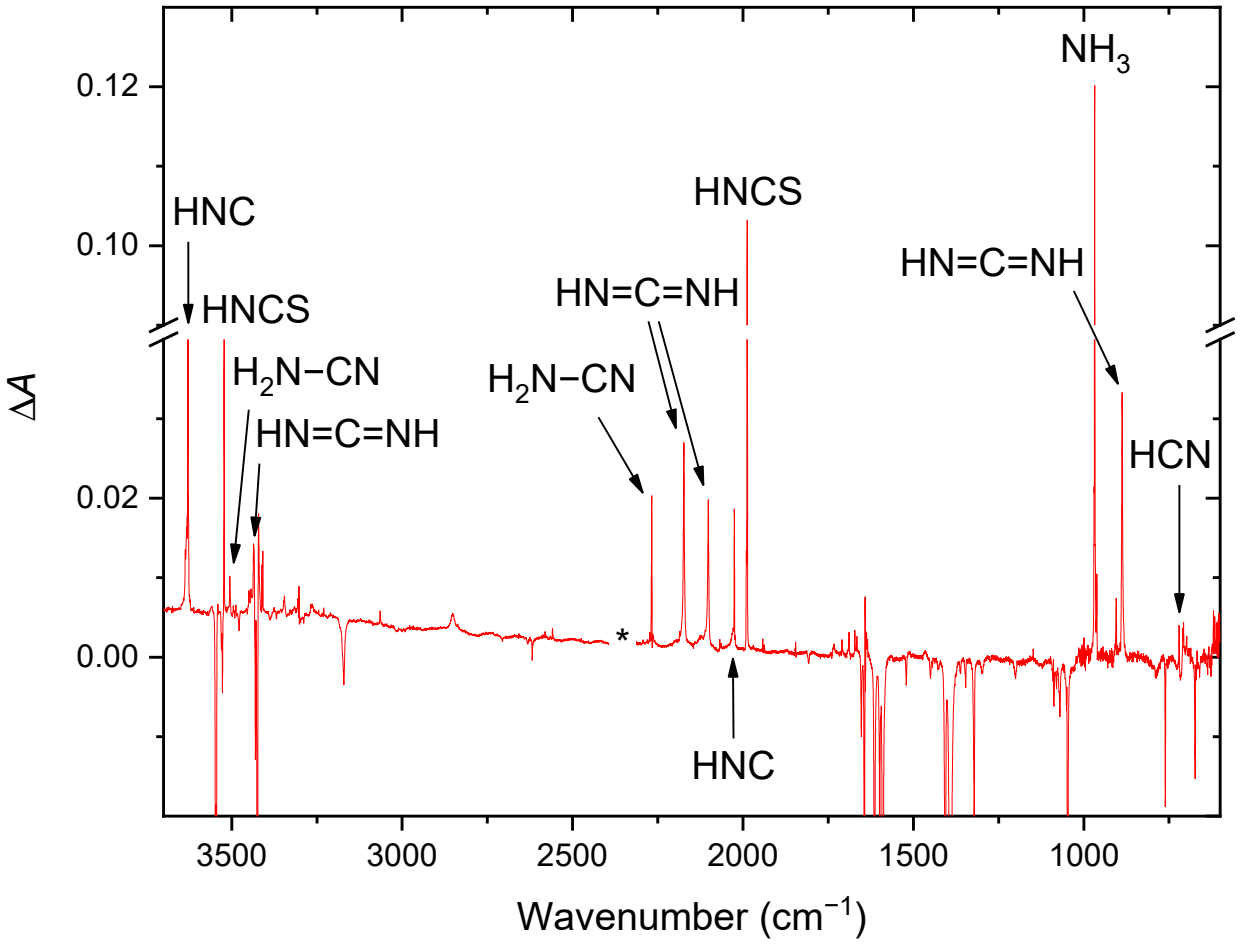

FIG. S3: Full-scale difference spectrum of the most prominent bands appearing after exposing TU to UV photons isolated in solid *para*-H_2. The band of gaseous CO_2 due to imperfect purge is marked with asterisks. The reference spectrum was the one taken right before the start of the 240 nm photolysis.

FIG. S4: Structures of the *a*- (left) and *s*-thione (right) tautomers of NMTU.

TABLE S4: The main experimental vibrational frequencies and intensities of *anti*-NMTU isolated in solid Ar and *para*-H_2 matrices as well as values obtained by theory.

Vibrational mode	**Ar**	***para*-H_2**	**Theor.**	
	$\tilde{\nu}^{a}$	$\tilde{\nu}^{a}$	$\tilde{\nu}^{b}$	I^{c}
$\nu_{as}(NH_2)$	3539.2	3548.3, <u>3546.2</u>	3564.1	46.2
ν(N–H)	<u>3485.8</u>, 3481.3	3480.9	3469.3	49.2
$\nu_{s}(NH_2)$	3423.3	3432.8, <u>3430.3</u>	3442.9	27.2
$\nu_{as}(CH_3)'$		3009.5	2980.0	10.0
$\nu_{as}(CH_3)''$		2919.3b, 2908.0b	2884.4	30.3
$\nu_{s}(CH_3)$		3009.5	2838.6	52.2
$\beta(NH_2)$	1595.7	1598.6	1587.8	150.7
β(N–H)	1520.1, 1509.4	1518.5sh, 1510.6	1490.9	340.7
$\beta_{as}(CH_3)'$	1475.7	1475.8	1473.7	14.9
$\beta_{as}(CH_3)''$	1453.7	1454.3	1456.6	20.2
$\beta_{as}(CH_3)''$			1452.4	12.0
$\beta_{s}(CH_3)$	1390.0	1389.7	1382.0	69.5
ρ(N–H)	1271.2b, 1265.5b	1267.6	1268.0	114.4
$\rho(CH_3)$	<u>1152.5</u>, 1148.3	<u>1152.2</u>	1139.0	19.7
ν(C–N)	1121.6	1123.5	1109.1	58.2
$\rho(NH_2)$	978.8	979.7	947.5	29.8
ν(C=S)	797.2	798.0b, 785.0b	781.0	10.6

[a] in cm^{-1}; b: broad; more intense components of split bands are underlined

[b] anharmonic vibrational frequencies in cm^{-1} as obtained at the B3LYP/cc-pV(T+d)Z level of theory

[c] harmonic vibrational intensities in km mol^{-1} as obtained at the B3LYP/cc-pV(T+d)Z level of theory

TABLE S5: The main experimental vibrational frequencies and intensities of *syn*-NMTU isolated in solid Ar and *para*-H_2 matrices as well as values obtained by theory.

Vibrational mode	**Ar**	***para*-H_2**	**Theor.**	
	$\tilde{\nu}^{a}$	$\tilde{\nu}^{a}$	$\tilde{\nu}^{b}$	I^{c}
$\nu_{as}(NH_2)$	3536.2	3538.4	3514.2	37.2
ν(N–H)	<u>3466.1</u>, 3456.9	3459.4	3439.6	18.5
$\nu_{s}(NH_2)$	3413.3	3419.4	3394.2	20.6
$\nu_{as}(CH_3)'$	3004.3	3000.9	2978.9	12.9
$\nu_{as}(CH_3)''$	2976.9	2970.3	2954.2	22.4
$\nu_{s}(CH_3)$	2956.1	2955.0	2920.5	38.1
–	2891.9	2891.1, 2860.0	–	–
$\beta(NH_2)$	1591.6	1595.2	1591.3	115.3
β(N–H)	1528.9	1528.2	1517.5	176.6
$\nu_{as}(CH_3)'$	1471.4	1471.4	1471.9	8.0
$\nu_{as}(CH_3)''$	1458.2, 1456.9	1458.9	1453.3	43.6
$\nu_{as}(CH_3)''$	1445.8, 1435.2	1447.0, 1436.6	1430.6	25.8
$\nu_{s}(CH_3)$	1374.7	1376.4	1364.8	156.8
ρ(N–H)	1302.8, 1291.3	1295.8b	1284.2	130.7
ν(N–CH_3)	1168.8	1167.2	1151.6	18.9
$\rho(CH_3))''$	–	–	1131.1	11.5
$\rho(CH_3))'$	1123.3	–	1119.5	8.5
–	1104.0	–	–	–
–	996.5	989.4b	–	–
$\rho(NH_2)$	965.7, 962.3	953.6	968.2	42.3
–	813.2		–	–
ν(C=S)	725.2	725.9	716.7	6.3
–	692.7	–	–	–
$\beta_{o.o.p.}$(NCN)	621.4	–	608.9	17.3

[a] in cm^{-1}; b: broad; more intense components of split bands are underlined

[b] anharmonic vibrational frequencies in cm^{-1} as obtained at the B3LYP/cc-pV(T+d)Z

level of theory

[c] harmonic vibrational intensities in km mol^{-1} as obtained at the B3LYP/cc-pV(T+d)Z level of theory

TABLE S6: The main experimental vibrational frequencies of the *a*,*s*,*t* and *s*,*s*,*t*-thiol conformers of NMTU isolated in solid Ar and *para*-H_2 matrices as well as values obtained by theory.

Conformer	**Vibrational mode**	**Ar**	***para*-H_2**	**Theor.**	
		$\tilde{\nu}$[a]	$\tilde{\nu}$[a]	$\tilde{\nu}$[b]	I[c]
a*,*s*,*t	**ν(C=NH)**	1633.5b	1636b	1642.8	209
s*,*s*,*t		1622.1	1623.5	1636.8	324

[a] in cm^{-1}; b: broad

[b] anharmonic vibrational frequencies in cm^{-1} as obtained at the B3LYP/cc-pV(T+d)Z level of theory

[c] harmonic vibrational intensities in km mol^{-1} as obtained at the B3LYP/cc-pV(T+d)Z level of theory

TABLE S7: The main experimental vibrational frequencies of the *s*,*t*-thiol conformer of NMTU isolated in solid Ar and *para*-H_2 matrices as well as values obtained by theory.

Vibrational mode	**Ar**	***para*-H_2**	**Theor.**	
	$\tilde{\nu}$[a]	$\tilde{\nu}$[a]	$\tilde{\nu}$[b]	I[c]
ν(C=N(–CH_3))	1657b	1656.7	1663.9	357

[a] in cm^{-1}; b: broad

[b] anharmonic vibrational frequencies in cm^{-1} as obtained at the B3LYP/cc-pV(T+d)Z level of theory

[c] harmonic vibrational intensities in km mol^{-1} as obtained at the B3LYP/cc-pV(T+d)Z level of theory

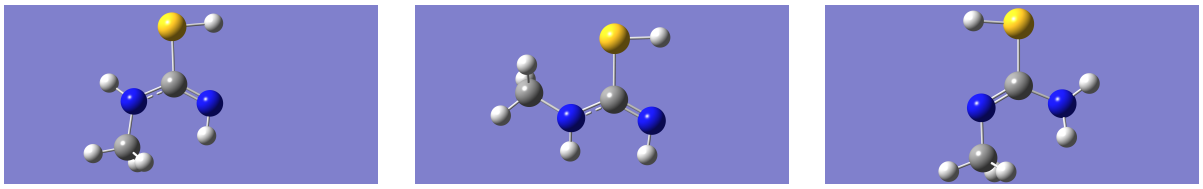

FIG. S5: Structures of the *a*,*s*,*t*- (left), *s*,*s*,*t*- (middle), and *s*,*t*-thiol (right) tautomers of NMTU.

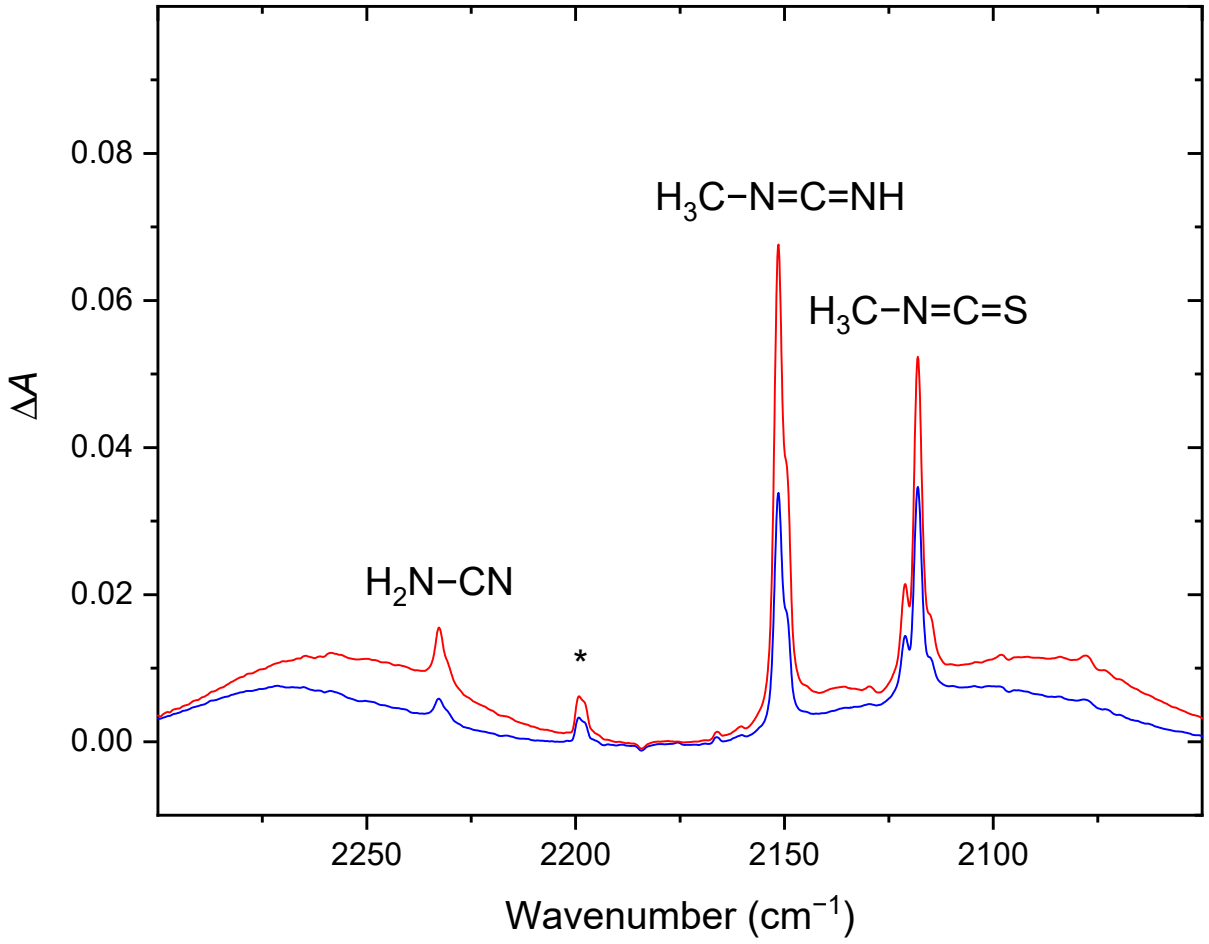

FIG. S6: Difference spectra of the most prominent bands appearing after exposing NMTU to 240 (blue trace) and 216 nm photons (red) isolated in solid Ar. The reference spectrum was the one taken right before the start of the 240 nm photolysis. The band marked with an asterisk can be assigned to the $\beta(H_3C–N=C)$ + $\nu(N=C)$ combinational vibration of $H_3C–N=C=S$ based on the computational results.

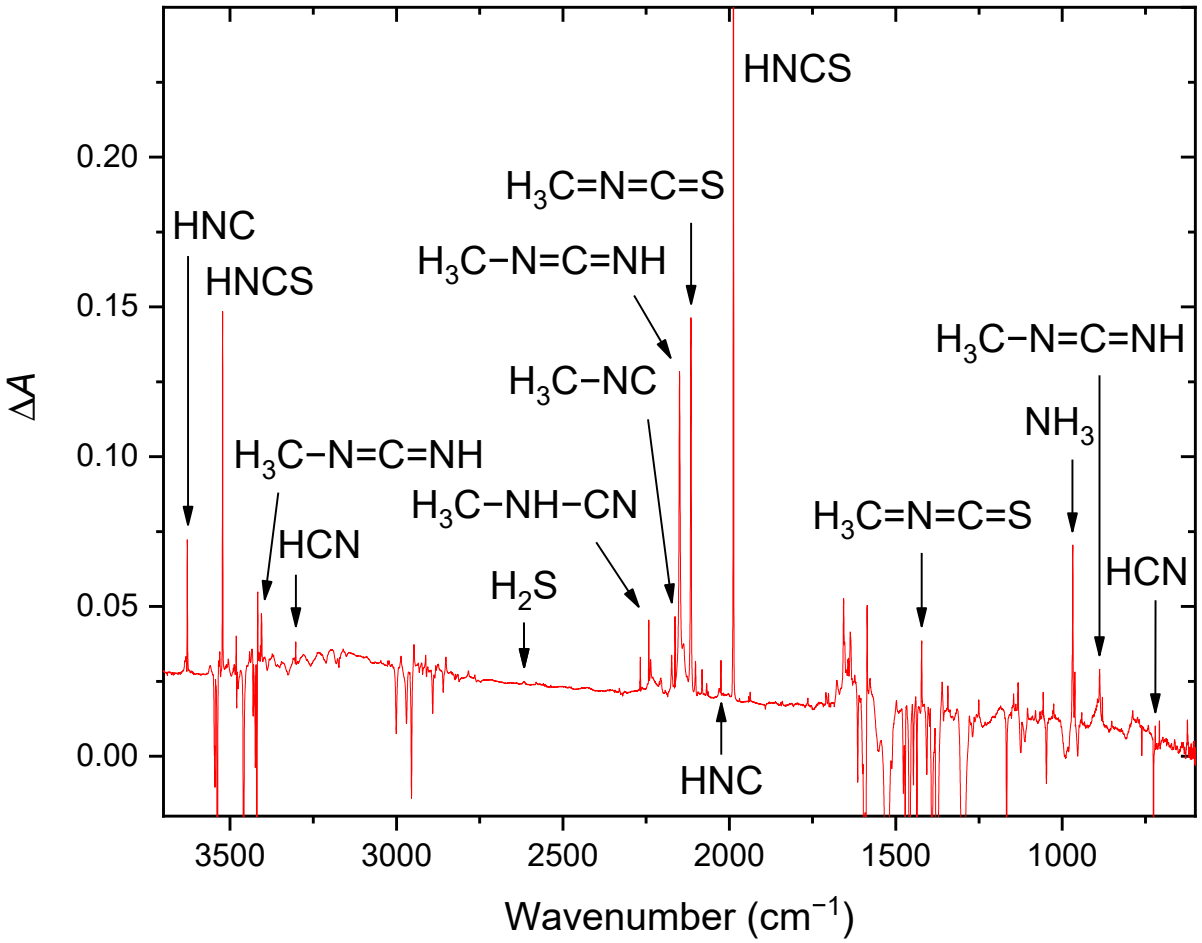

FIG. S7: Full-scale difference spectrum of the most prominent bands appearing after exposing NMTU to UV photons isolated in solid *para*-H_2. The reference spectrum was the one taken right before the start of the 240 nm photolysis. Note that some bands of TU and its irradiation products can be observed due to TU impurity in the sample in this experiment.

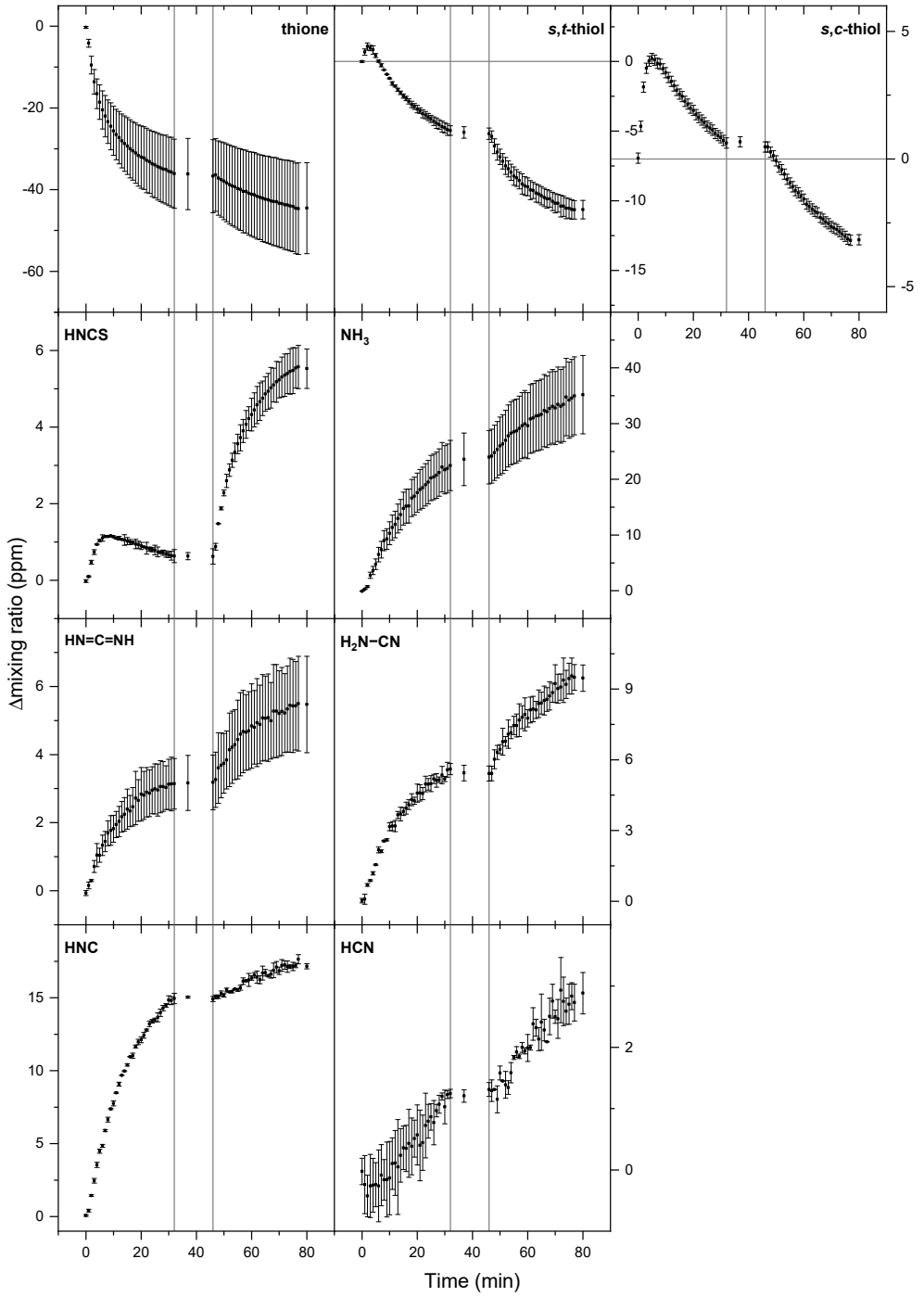

FIG. S8: Kinetic curves of TU and the products belonging to the laser UV photolysis. The horizontal lines on the panels showing the thiol tautomers mark the zero reference point, whereas the vertical lines at 32 and 46 minutes on each panel mark the time period when the irradiation was paused when switching from 240 nm to 216 nm.

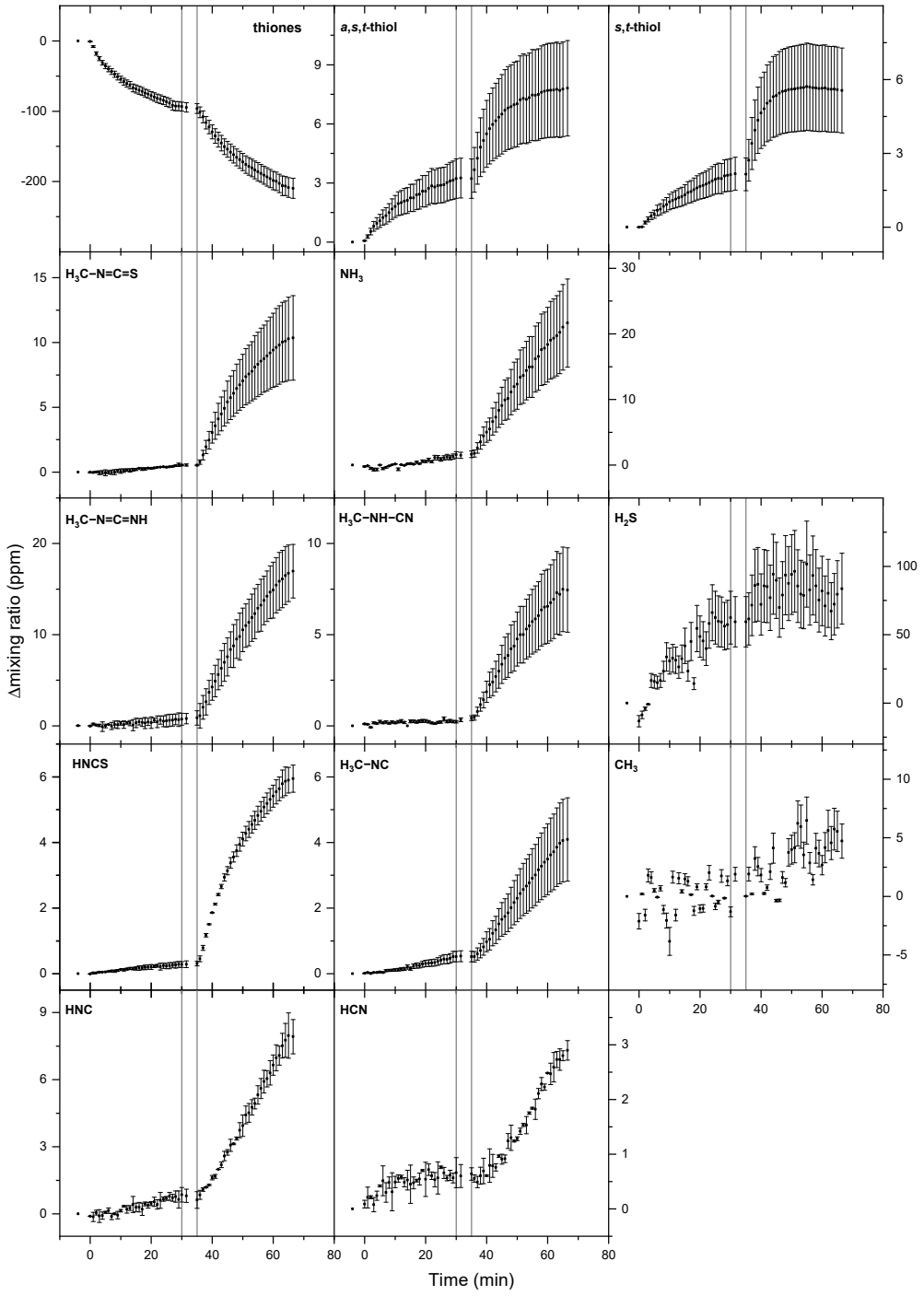

FIG. S9: Kinetic curves of NMTU and the products belonging to the laser UV laser photolysis. The vertical lines at 30 and 35 minutes into the irradiation on each panel mark the time period when the irradiation was paused when switching from 240 nm to 216 nm.

REFERENCES

[1]H. Rostkowska, L. Lapinski, A. Khvorostov, and M. J. Nowak, "Proton-transfer processes in thiourea: UV induced thione → thiol reaction and ground state thiol → thione tunneling," The Journal of Physical Chemistry A **107**, 6373–6380 (2003).

[2]H. Rostkowska, L. Lapinski, and M. J. Nowak, "Hydrogen-atom tunneling through a very high barrier; Spontaneous thiol → thione conversion in thiourea isolated in low-temperature Ar, Ne, H_2 and D_2 matrices," Physical Chemistry Chemical Physics **20**, 13994–14002 (2018).